

Square Wave Voltammetric Detection of Dimethylvinphos and Naftalofos in Food and Environmental Samples Using RGO/CS modified Glassy Carbon Electrode

P.ReddyPrasad¹, A.E.Ofamaja¹, C.Nageswara Reddy² and E.B.Naidoo^{1,*}

¹ Department of Chemistry, Vaal University of Technology, P. Bag X021, Vanderbijlpark-1900, South Africa.

² Department of Chemistry, Govt. Degree College, Koduru, Kadapa, A.P, India.

*E-mail: bobby@vut.ac.za

Received: 19 August 2015 / Accepted: 19 November 2015 / Published: 1 December 2015

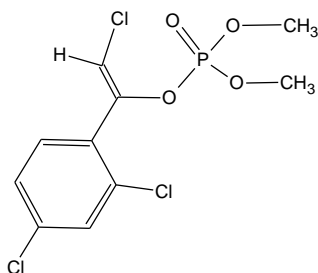
A novel modified reduced graphene oxide (RGO)/chitosan (CS) on a glassy carbon electrode for the determination of dimethylvinphos (2-chloro-1-(2,4-dichlorophenyl)vinyl dimethyl phosphate) and naftalofos (O,O-Diethyl-N-hydroxynaphthalimide phosphate) has been developed. The modified RGO/CS/GCE film was studied by cyclic voltammetry, square wave voltammetry and transmission electron microscopy. The effects of deposition potential, deposition time, scan rate, square wave frequency and pulse amplitude were examined to optimize the conditions of square wave voltammetry. The RGO/CS/GCE was well accomplished and determined in the range of 0.05–30.0 $\mu\text{g L}^{-1}$ for dimethylvinphos and naftalofos. The detection of limit (3Sb/S) was calculated and found to be 0.036 mg L^{-1} for dimethylvinphos and 0.044 mg L^{-1} for naftalofos with RGO/CS/GCE. The proposed sensor was successfully applied to food and environmental samples.

Keywords: Dimethylvinphos, naftalofos, graphene oxide, chitosan, food and environmental samples.

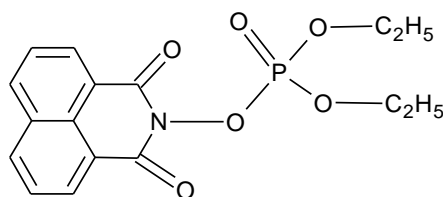
1. INTRODUCTION

Organophosphorus pesticides (OPs) are esters of phosphorous based acid derivatives that have been widely used for pest control in agriculture due to their high insecticidal activity, acute toxicity and relatively short environmental persistence [1–4]. Since, these Ops are prohibition in the last decade, its application in the environment is constantly decreasing. However, they are main pesticides in many developing countries [5]. Dimethylvinphos and naftalofos are systemic and general OPs [6] (structure I). These organic toxins may enter animals and humans directly or indirectly through the food chains [7, 8]. Because of their high toxicity, it is necessary to develop reliable analytical procedures for their determination in trace amounts in the environment. From literature studies, several

methods have been developed for the determination of OPs by various analytical techniques such as gas chromatography, high performance liquid chromatography, spectrophotometry and electroanalytical techniques [9-19].



Dimethylvinphos



Naftalofos

Structure I. Chemical structures of dimethylvinphos (DMV) and naftalofos (NTF)

Currently carbon modified electrodes are broadly used in electro-analysis because of their low background currents, wide potential gap, chemical inertness, economical, suitability for several sensing and detection procedures [20,21]. Since the discovery of graphene (GR) [22] various investigations have focused on the studies of their properties and applications [23-27]. Most of the graphene applied in electrochemistry studies are produced from the reduction of GO, and usually contain functional groups such as hydroxyl and carboxyl which are advantageous for electrochemical applications [28-33]. However, the chitosan (CS) is a linear biopolymer and commercially produced by deacetylation of chitin. Chitosan is an interesting bio-polymer due its following characters such as bio-adhesive, biocompatible, biodegradable, good mechanical strength, readily soluble in water and non-hazardous [34]. CS has been widely used to construct a good biocompatible electrochemical sensors [35]. But not much attention has been given to understand the RGO/CS/GCE modified electrode performance of the compounds of interest by square wave voltammetry. This approach is facile and green and does not involve toxic reductant, while the resultant composite is clean and requires no further dispersant.

In this work, a novel electrochemical sensor of RGO/CS/GCE was developed that is environmentally friendly for the detection of OPs. The modified electrode is reported as efficient method for the reduction of graphene oxide using chitosan (CS) as stabilizer. The electrochemical sensor is examined by transmission electron microscopy, cyclic voltammetry and square wave voltammetry. This novel electrochemical sensor can be applied for sensitive determination of DMV

and NTF in food and environmental samples by square wave voltammetry. The results shows that modified RGO/CS/GCE exhibits good performance for detecting of DMV and NTF.

2. EXPERIMENTAL

2.1. Instrumentation and reagents

The electrochemical investigation were performed with Autolab PG STAT101 supplied by Metrohm Autolab B.V. Netherlands. A conventional three electrode system which include glassy carbon electrode as working electrode, Ag/AgCl (salt KCl) as a reference electrode and a platinum wire as an auxiliary electrode. Transmission electron microscopy (TEM) illustration have been executed on JEM-100CXG and Philips Tecnai F20 electron microscope. An Elico Li-129 model glass-calomel combined electrode was employed for measuring pH values. All chemicals used were of analytical reagent grade and used without additional purification. All solutions were prepared with Millipore milli-Q nanopore water (resistivity $\geq 18 \text{ m}\Omega \text{ cm}^{-1}$). Graphene, chitosan and Briton-Robinson (BR) buffer were purchased from Sigma Aldrich, India. The analytical technical grade samples of DMV and NTF insecticides in the form of 50% wet table powders were obtained from Bayer India Ltd., India. All experiments had been performed at room temperature ($\sim 25 \text{ }^\circ\text{C}$).

2.2. Fabrication of modified RGO/CS/GCE

Prior to electrodeposition, the GCE was polished with specific grades of $0.3 \mu\text{m}$ and $0.05 \mu\text{m}$ $\alpha\text{-Al}_2\text{O}_3$ powders till a mirror-shiny surface was obtained, then ultra-sonicated in ethanol and distilled water for 15 min, respectively. The prepared GCE was dried with nitrogen gas and used for modification immediately. Then, 4.0 mg of GO was dispersed in 5 mL of 0.2% (w/v) CS solution with ultra-sonication to form $0.8016 \text{ mg mL}^{-1}$ GO/CS solution. The shiny GCE was immersed into the GO/CS solution while stirring at fixed potential of -1.0 V for 100 s. The RGO/CS/GCE was stored at $\sim 4 \text{ }^\circ\text{C}$ in a refrigerator under dry conditions when not in use. For comparison, CS/GCE was acquired by electrodepositing CS onto the GCE under -1.0 V for 100 s.

2.3. Recommended analytical procedure for the determination of DMV and NTF

An aliquot of working standard solution containing $0.12\text{-}10 \mu\text{g mL}^{-1}$ of DMV and NTF were transferred into 25 mL volumetric flask. To this 10 mL of BR buffer of (pH 6.0) was transferred into voltammetric cell and then deoxygenated with nitrogen gas for 15 min. The DMV and NTF pesticides were determined in the square wave mode. Electrolysis was done at -0.14V to -1.0 V vs SCE, deposition potential -0.32V , deposition time 100 s, scan rate 20 mVs^{-1} , square wave frequency 60 Hz, pulse amplitude 50 mV and pH 6.0. For DMV and NTF samples the maximum square wave peaks appears at -0.39 and -0.66 V respectively.

3. RESULTS AND DISCUSSION

The modified GCE with RGO is not very stable as a result of its poor van der Waals attraction forces. On the other hand, CS biopolymer with many amino groups along its macromolecular chains can interact strongly with hydroxyl and carboxylic groups on its surface of RGO [36, 37]. Hence, CS can act as a binder to stabilize the RGO on GCE. The CS biopolymer is positively charged in aqueous solutions with pH values lower than 6.0. However, as the pH of the solution increases, the charged amino groups (NH_3^+) becomes deprotonated and thus, insoluble. This issue opens a way for electrodeposition of CS at the electrode surface. Electrodeposition of chitosan was performed using various concentrations of (0.01-0.4% w/w) chitosan solutions at pH 6.0. Considering both the sensitivity and the stability of the electrode, response showed that 0.2% (w/v) CS is the optimum concentration for the construction of RGO/CS/GCE electrochemical sensor. The effect of the amount of GO and the pH of solution were also investigated from which the value of 4.0 mg and the pH 6.0 obtained were to be the most appropriate conditions for the electrodeposition of RGO.

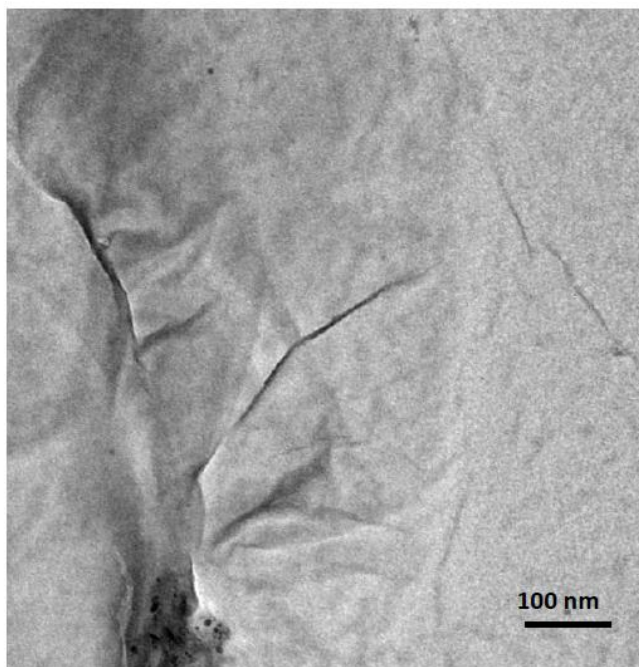


Figure 1. TEM illustration of the electrodeposited RGO/CS composite on the GCE

Fig. 1 shows the TEM image of the RGO/CS composite electrodeposited on the GCE surface, illuminating the typical crinkly and wrinkled RGO nanosheet structure on the rough surface of the CS/GCE. This wrinkled nature of RGO are ultrathin transparent nanosheets and incredibly useful in keeping an excessive surface on the electrode surface and facilitate the diffusion of the analyte. This results indicates that RGO/CS nanocomposite was successfully coated on GCE from RGO/CS dispersion by direct one-step electrodeposition.

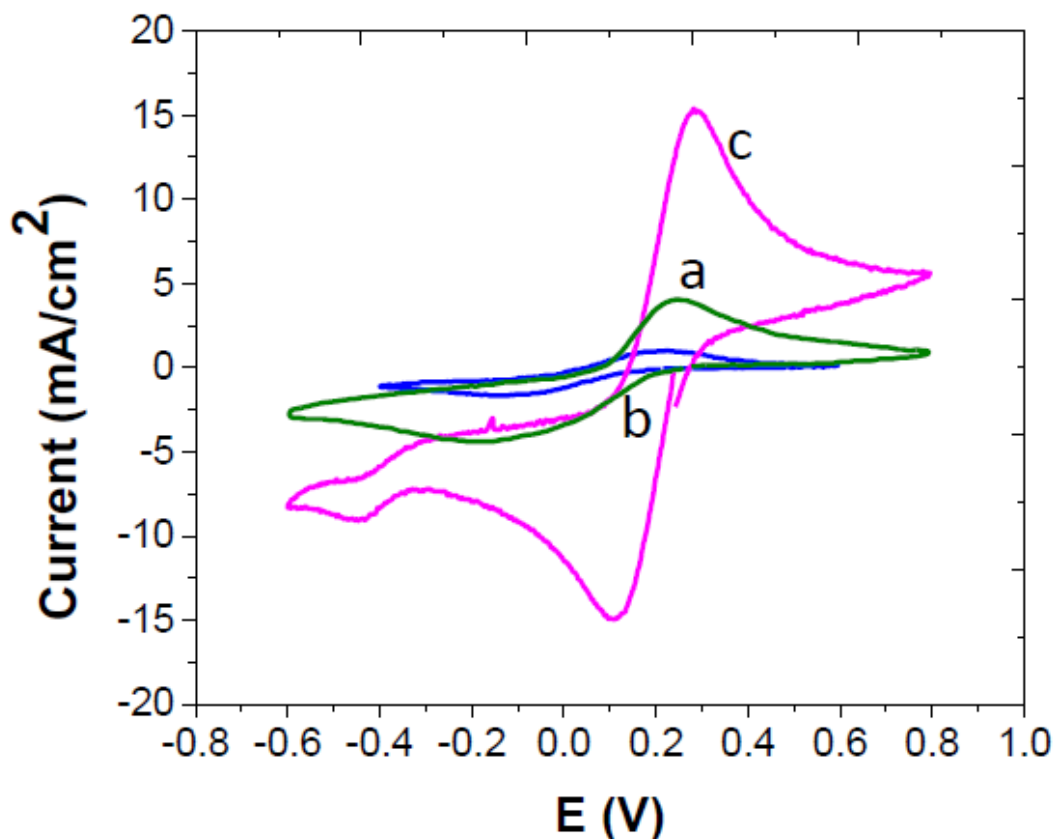


Figure 2. Typical cyclic voltammogram of bare GCE(a), CS/GCE (b) and RGO/CS/GCE (c) in 5.0 mM $[\text{Fe}(\text{CN})_6]^{3-/4-}$ containing 0.1 M KCl at 20 mV s^{-1} , at pH 6.0, accumulation time: 100 s; accumulation potential: -0.32V ; concentration of OPs: $4.0 \mu\text{g mL}^{-1}$.

Fig. 2 shows the cyclic voltammograms obtained by modified GC electrode in a 5.0 mM $[\text{Fe}(\text{CN})_6]^{3-/4-}$ containing 0.1 M KCl at 20 mV s^{-1} scan rate. As shown, a pair of well-defined cyclic voltammogram was observed for the bare GC electrode, which was due to the reversible one-electron redox behaviour of ferricyanide ion (Fig. 2, curve a). After electrodeposition of CS onto the bare GCE, a blocked interfacial charge transfer between the bare GCE and ferricyanide ion was observed (Fig. 2, curve b), because of CS layer which acts as a barrier. Compared with bare CS/GCE or even the bare GCE surface, increased redox peak currents were observed with RGO/CS/GCE (Fig. 2, curve c), indicating that RGO enables the conductivity and the electron transfer process.

The electrochemical behaviors of $4.0 \mu\text{g mL}^{-1}$ of DMV and NTF on the bare GCE, CS/GCE, and RGO/CS/GCE were investigated using cyclic voltammetry. DMV and NTF exhibits two redox cyclic voltammetric peaks over the pH range of 3.0 to 10.0. These peaks were attributed to the reduction of $>\text{C}=\text{C}<$ (DMV), $>\text{C}=\text{O}$ (NTF) groups involving two and four electrons each respectively. The irreversible reduction peaks corresponding to the reduction of $>\text{C}=\text{C}<$, $>\text{C}=\text{O}$ groups were attributed to two and four electron transfer process, which is consistent with the literature [36]. There is no characteristic reduction peak in basic medium ($8 \leq \text{pH} \leq 12$) for $>\text{C}=\text{C}<$, $>\text{C}=\text{O}$ groups due to the precipitation of electroactive species (Fig. 3.).

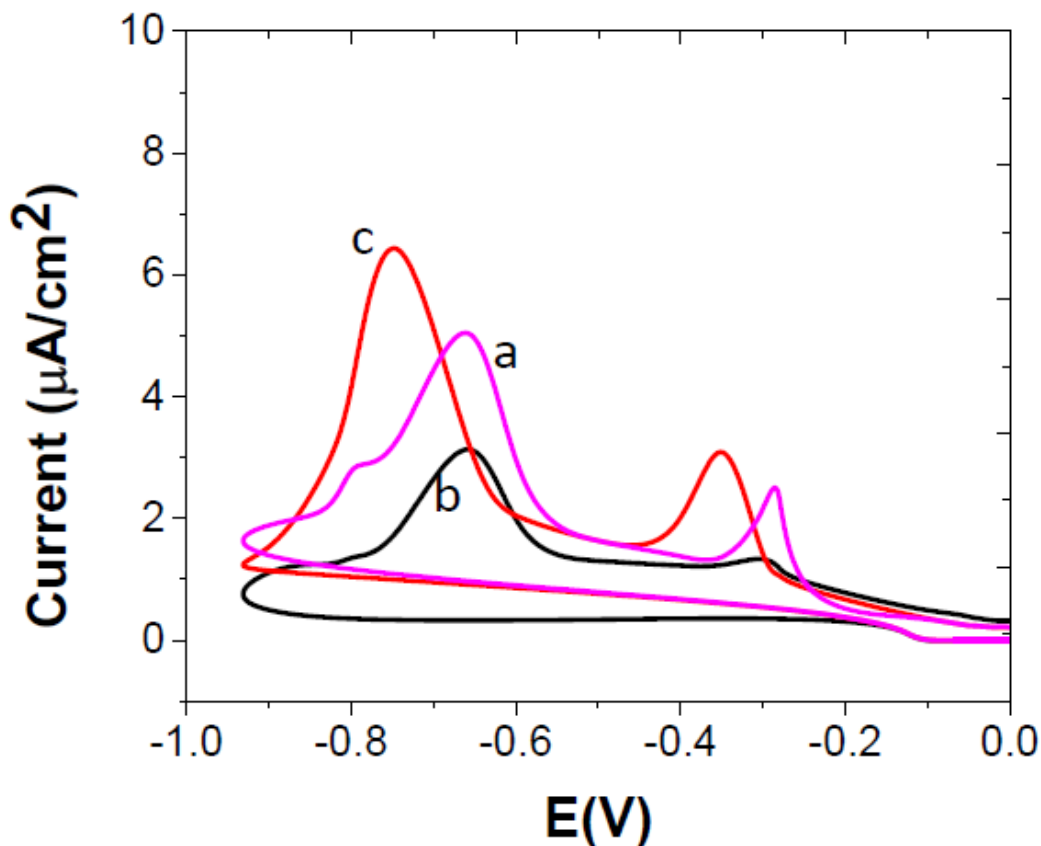


Figure 3. Cyclic voltammograms of DMV, NTF at bare GCE (a), CS/GCE (b) and RGO/CS/GCE (c), accumulation time: 100 s; pH: 6.0; accumulation potential: -0.32 V; scan rate: 20 mVs⁻¹, concentration of OPs: 4.0 μg mL⁻¹.

Compared with bare GCE (Fig.3, curve a) CS/GCE (Fig.3, curve b), the cyclic peak currents of DMV and NTF increased with the RGO/CS/GCE (Fig.3, curve c). Based on the results, the following conclusions can be drawn: firstly, the DMV and NTF were strongly attached on to RGO/CS/GCE film indicating good adsorption; secondly, the sensitivity of the RGO/CS sensor towards DMV and NTF was significantly enhanced due to the exceptional electric conductivity and the large surface area of RGO.

Fig. 4 shows a comparison between the square wave voltammetry signals of bare GCE, CS/GCE and RGO/CS/GCE for 4.0 μg mL⁻¹ DMV and NTF in 0.1 M BR buffer solution (pH 6.0) respectively. A low intensity of peak current was observed on bare GCE in BR buffer (Fig.4, curve a), comparison of CS/GCE (Fig 4, curve b) and RGO/CS/GCE (Fig 4, curve c) respectively. In comparison, square wave voltammetry peak on OPs/RGO/CS/GCE was much higher than with OPs/CS/GCE at potential range from -0.14V to -0.98 V. Based on the above results the electrochemical study was carried out by RGO/CS/GCE. Hence, the RGO/CS/GC modified electrode exhibited well defined peaks at -0.39 V, -0.66 V for DMV and NTF respectively.

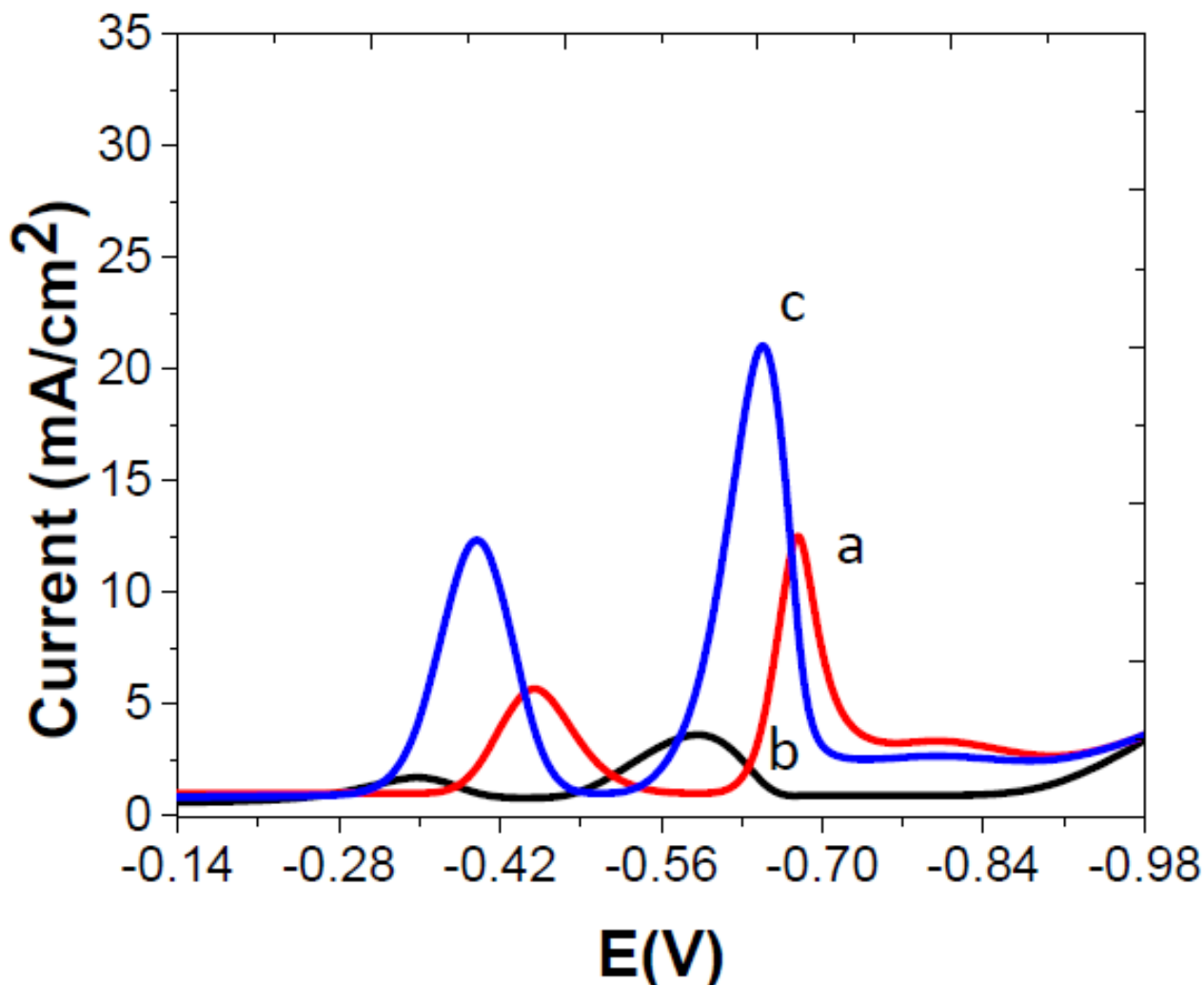


Figure 4. Square wave voltammograms of DMV and NTF at bare GCE (a), CS/GCE (b) and RGO/CS/GCE (c), accumulation time: 100 s; pH: 6.0; accumulation potential: -0.32 V; scan rate: 20 mVs⁻¹, square wave frequency 60 Hz; pulse amplitude 50mV; concentration of OPs: 4.0 $\mu\text{g mL}^{-1}$.

3.1. Effect of optical parameters for square wave voltammetry

The optimization of the square wave voltammetry parameters that can influence the current response of analyte is a significant step in the extension of the voltammetric procedure. Hence, the optimum experimental limitations such as solution pH, deposition potential, deposition time, square wave frequency, scan rate and pulse amplitude have been examined in this study. The optimization process was carried by changing each parameter at a time while the others were kept constant. Solution pH is one of the important parameter in electrochemical characterization of the analytes. The pH was investigated in the range of 3.0-10.0 and the maximum peak was obtained in BR buffer of pH 6.0 (Fig. 5). As a result, the BR buffer pH 6.0 was used as supporting electrolyte.

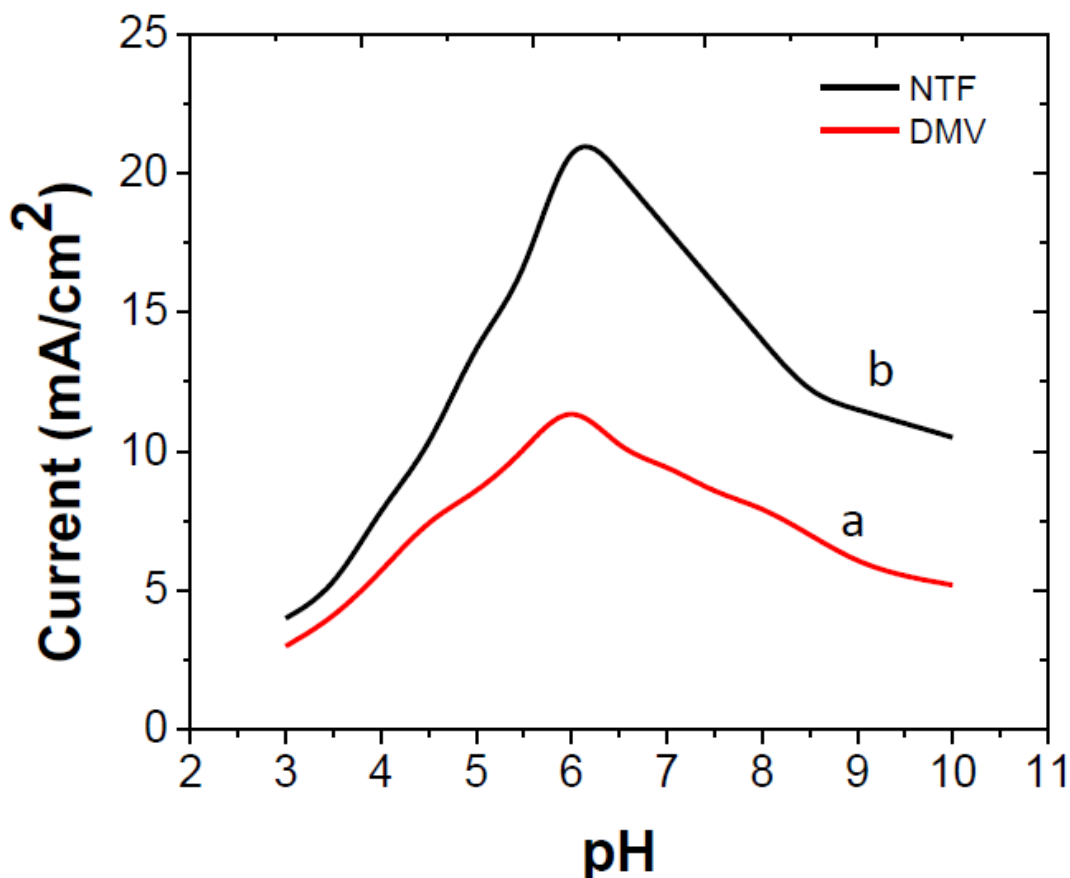


Figure 5. Effect of pH on DMV (a) and NTF (b) solution at RGO/CS/GCE, accumulation time: 100 s.; accumulation potential: -0.32V; square wave frequency 60 Hz; pulse amplitude 50mV; concentration of OPs: $4.0 \mu\text{g mL}^{-1}$, scan rate: 20 mVs^{-1} .

At $\text{pH} < 6.0$, the reduction of hydronium ion (H_3O^+) may cause the decrease in intensity of peak current. At $\text{pH} > 6.0$, the decomposition of DMV and NTF comes sensitive reduction. The influence of the deposition potential on the square wave voltammetry signal was studied with accumulation time of 100 s, at RGO/CS/GCE for $4.0 \mu\text{g mL}^{-1}$ DMV and NTF respectively. From, Fig. 6 an accumulation potential value of -0.32V at pH 6.0 was observed due to its increase in accumulation rate. This provides more favorable accumulation potential, pH for the electric field at the electrode solution interface between RGO/CS on GCE. The dependence of the peak on the accumulation time t_{acc} (sec), on the square wave peak current of the DMV and NTF in BR buffer of pH 6.0 was investigated and shown in Fig.7. The accumulation time of 100 s at -0.32 V have been generated a stronger peak current. As for the scan rate, the current response increases with the increasing scan rate of 20 mVs^{-1} . Consequently, the optimum conditions for recording a maximum and sharp square wave voltammetric peak for $4.0 \mu\text{g mL}^{-1}$ pesticide residues was at scan rate: 20 mVs^{-1} . It was determined that the peak current of both pesticides increased as the modulation was rising from 20 to 100 mV accompanied by the broadening peak width. When the amplitude was higher than 50 mV, the peak current become much wider. The variation of frequency was studied in the range of 10-100 Hz with level of change of 10 Hz each time. The peak current of OPs increases with frequency up to 100 Hz, above which it was unstable as well as large current fluctuations were observed. For the reason, frequency of 60 Hz in

study was compromised. In order to show the validation of the proposed method, the square wave stripping voltammetric response on the RGO/CS/GCE electrochemical sensor from concentrations of DMV or NTF was recorded using the optimized conditions as shown in Table 1.

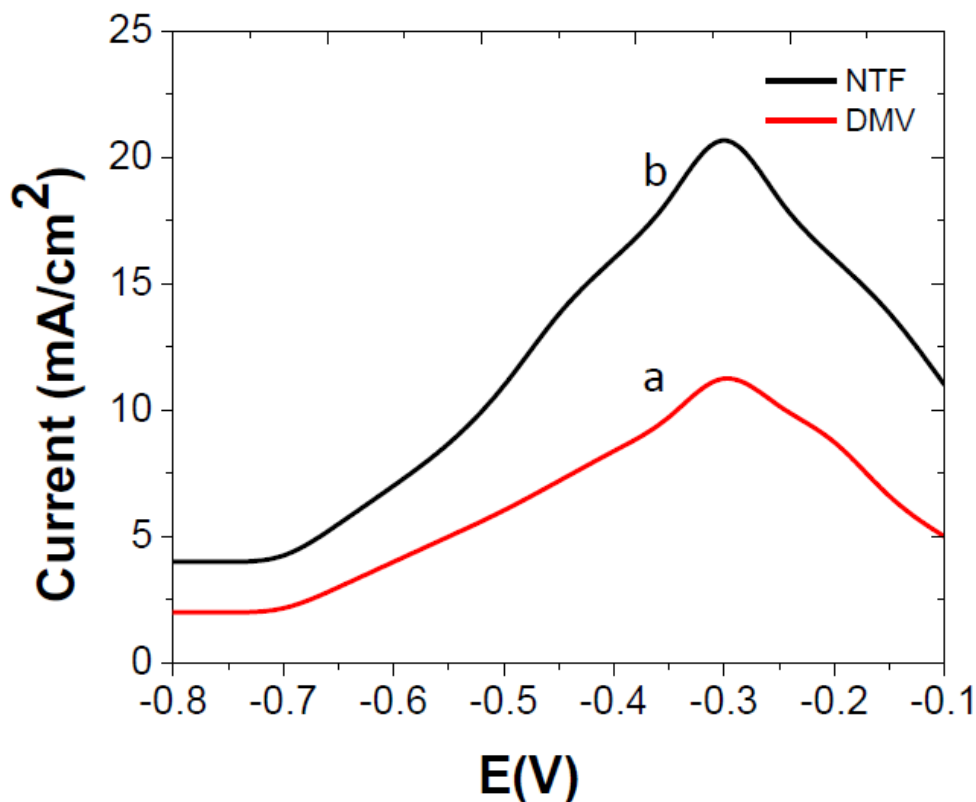


Figure 6. Effect of accumulation potential on the square wave voltammetry of DMV (a) and NTF (b) at pH 6.0, concentration of OPs: $4.0 \mu\text{g mL}^{-1}$; accumulation time: 100 sec; square wave frequency 60 Hz; pulse amplitude 50mV; scan rate: 20 mV s^{-1} .

Table 1. Optimal operational parameters selected from the univariate analysis

Optimized parameters	Value
Graphene	4.0 mg
Chitosan	0.2% (w/v)
Supporting electrolyte	BR buffer
pH	6.0
Deposition potential	-0.32 mV
Deposition time	100 s
Scan rate	20 mVs^{-1}
SW frequency	60 Hz
SW amplitude	50 mV

3.2. Effect of interfering ions

Table 2. Effect of various pesticides and pollutants ($5.0 \mu\text{g mL}^{-1}$ in 25 mL)

Interfering species	Tolerance limit ($\mu\text{g mL}^{-1}$)	Interfering species	Tolerance limit ($\mu\text{g mL}^{-1}$)
BHC, DDT	800	Ca(II), Mg(II)	400
Benzene, ether	360	Cu(II), Pb(II), Co(II)	250
Chloroform	400	NO_2^-	160
Malathion, Phorte,	380	NO_3^-	120
Quinolpos			
Dichlorvos	350	SO_4^-	100
Bifenthrin	300		
parathion	200		
Toluene, Dimethoate	100		

To evaluate the interference effect on the determination of DMV and NTF at the $4.0 \mu\text{g mL}^{-1}$, a systematic study was carried out. Known amounts of interfering species and pesticides were added to the standard solution containing $4.0 \mu\text{g mL}^{-1}$ of DMV and NTF, then analyzed by the proposed method. The other pesticides such as malathion, fenitrothion, 2,4-D and parathion methyl did not interfere strongly. The limits of tolerance and the concentrations of diverse species that cause $\pm 2.5\%$ error in the determination of DMV and NTF by this method were given in Table 2. These results showed that a large number of metallic and non-metallic ions did not interfere with the analysis of DMV and NTF.

3.3. Analytical applications

Table 3. Recoveries of DMV and NTF in food samples

Samples ^a	Pesticide	Added ($\mu\text{g mL}^{-1}$)	Found ($\mu\text{g mL}^{-1}$) ^b	Recovery (%)	Standard Deviation
Tomato	DMV	10.0	9.98	99.80	0.06
		20.0	19.96	99.80	0.02
	NTF	10.0	9.96	99.60	0.01
		20.0	19.99	99.95	0.12
Potato	DMV	10.0	9.99	99.90	0.02
		20.0	19.80	99.00	0.11
	NTF	10.0	9.95	99.50	0.04
		20.0	19.98	99.90	0.08

^aCollected from local market, Tirupati; (n=5)^b

Food (Tomato and Potato) samples were collected from an agricultural field, where DMV and NTF had been spiked as an OPs. 25.0 g of sample was then soak with two 20 mL portions of ethanol-

demineralized water (1+1), filtered through a Whatman filter paper No.41 and filtrate was centrifuged at 4000 rpm for 10 min. The filtrate was quantitatively transferred into a 50 mL calibrated flask and made up to the mark with 50% ethanol. Washings were collected in a 25 mL calibrated flask and aliquots were analyzed as per to the recommended procedure. The obtained results for the determination of the DMV and NTF in food samples are summarized in Table 3. Recoveries of DMV and NTF obtained are in the range from 99.00 to 99.95%, which shows the accuracy and reproducibility of the recommended method.

Table 4. Determination of DMV and NTF in water samples

Samples ^a	Pesticides	Added ($\mu\text{g mL}^{-1}$)	Found ($\mu\text{g mL}^{-1}$) ^b	Recovery (%)	Standard Deviation
Rice-field water	DMV	10	9.98	99.80	0.06
		20	19.88	99.40	0.02
	NTF	10	9.97	99.70	0.14
		20	19.99	99.95	0.10
River water	DMV	10	9.95	99.50	0.04
		20	19.97	99.90	0.02
	NTF	10	9.94	99.85	0.11
		20	19.985	99.25	0.18

^aCollected from Nellore(Dist), ^b(n=5)

Table 5. Comparisons of the response of RGO/CS/GCE for detection of OPs with other modified electrodes

S.No	Modified Electrode	Supporting electrolyte	Method	Linear range	Detection limit	Ref.
1	Poly(malachite green)/graphene-NF ^a	PBS, pH 5.0	amperometry	$2 \times 10^{-8} - 1.5 \times 10^{-6}$ M	2.00×10^{-10} M	38
2	Graphene/Gold nanoparticles	PBS, pH 5.7	SWV	$6.85 \times 10^{-10} - 3.43 \times 10^{-9}$ M	2.05×10^{-12} M	39
3	Cyclodextrin/Graphene	PBS, pH 7.0	DPV ^b	$3.43 \times 10^{-9} - 1.71 \times 10^{-6}$ M	1.71×10^{-10} M	40
4	ZrO ₂ /graphene	KCl, pH 5.2	SWV	$6.86 \times 10^{-12} - 3.08 \times 10^{-9}$ M	2.00×10^{-12} M	41
5	^a NF/AchE ^c -CS/SnO ₂ NPs-CGR ^d -NF	PBS, pH 7.4	amperometry	$10^{-12} - 10^{-10} / 10^{-10} - 10^{-8}$ M	5.00×10^{-13} M	42
6	RGO/CS	BR, pH 6.0	SWV	0.05–30.0 $\mu\text{g L}^{-1}$	0.036/0.044 $\mu\text{g L}^{-1}$	Present work

^anafion; ^bdifferential pulse voltammetry; ^cacetylcholinesterase; ^dcarboxylic graphene

The determination of DMV and NTF in water samples from Rice-field water and Penna River, India, were carried out using the RGO/CS/GCE. Before analysis, the water samples were centrifuged at 4000 rpm to remove the solid impurity and the pH was adjusted to 6.0 with the addition of BR buffer. The obtained water samples without addition of DMV and NTF did not show the signals of analytes and consequently, the determination of the DMV and NTF concentration were performed using the standard addition approach. The results of different concentrations detected by square wave voltammetric method was listed in Table 4. It is found that the results obtained by square wave voltammetry was in good agreement with the actual addition with the recovery from 99.25 to 99.95%, indicating potential for practical DMV and NTF detection. The obtained results indicate that the recommended method is reliable and it has potential for practical application.

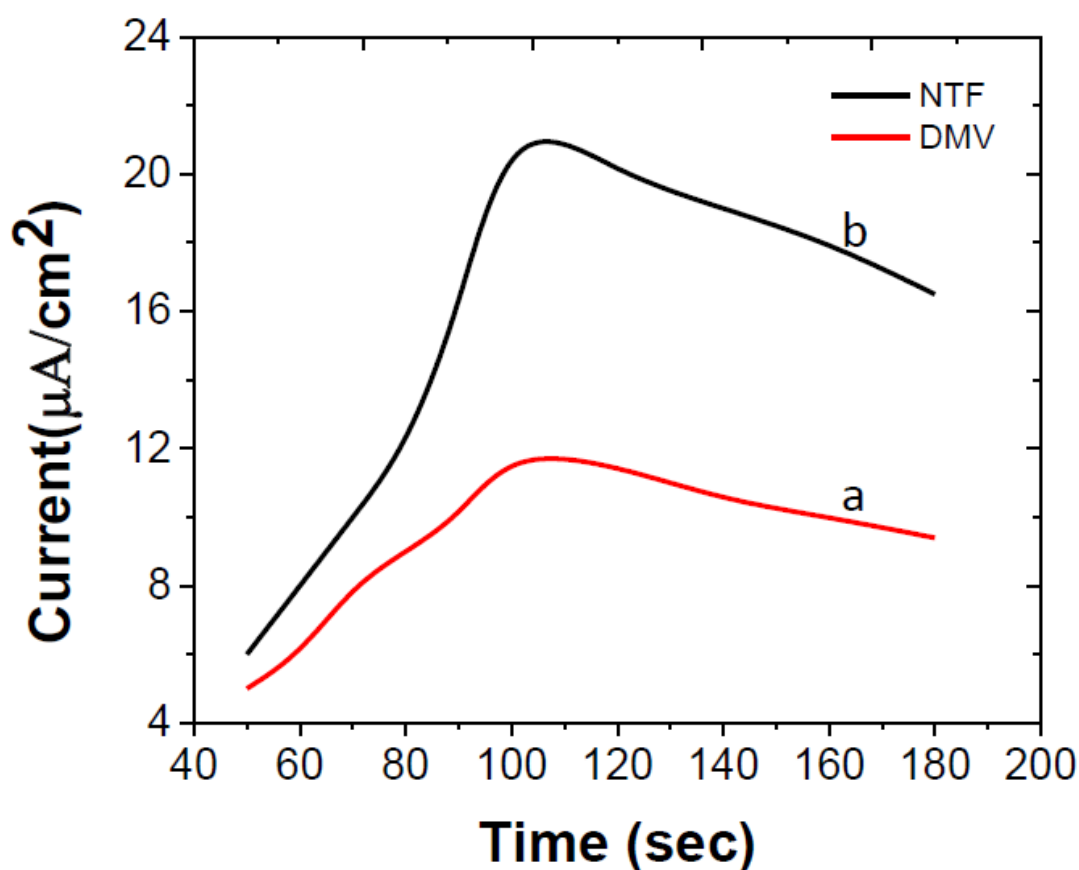


Figure 7. Effect of accumulation time on the square wave voltammetry of DMV(a) and NTF (b) at pH 6.0, concentration of OPs: $4.0 \mu\text{g mL}^{-1}$; accumulation potential: -0.32 V ; square wave frequency 60 Hz; pulse amplitude 50mV; scan rate: 20 mV s^{-1} .

Table 5 summarizes the assessment of some of the analytical parameters used for OPs in this study with those earlier described methods. As it can be seen, the constructed modified electrode was superior in some cases as compared to the earlier reported modified electrodes.

3.4. Calibration graph

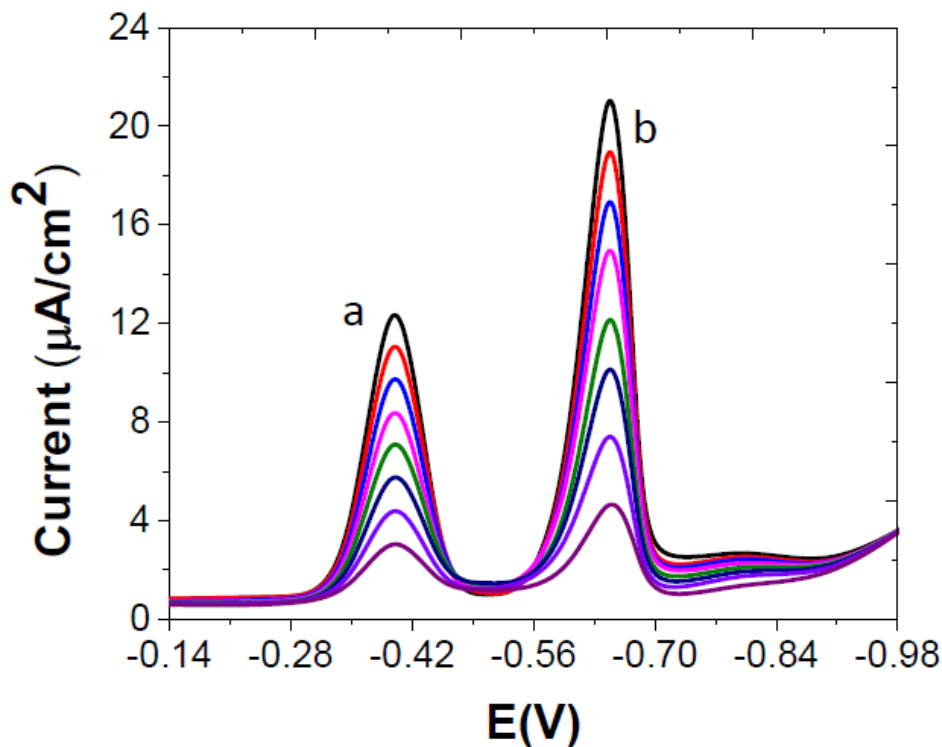


Figure 8. Square wave voltammetry responses of RGO/CS/GCE in a BR buffer at pH 6.0 after incubation with 0.2 (a), 4.0 (b), 8.0 (c), 12.0 (d), 16.0 (e), 20.0 (f), 24.0 (g), 30.0 (h) $\mu\text{g mL}^{-1}$ of DMV (a) and NTF (b), accumulation potential: -0.32 V; square wave frequency 60 Hz; pulse amplitude 50mV; scan rate: 20 mV s^{-1} .

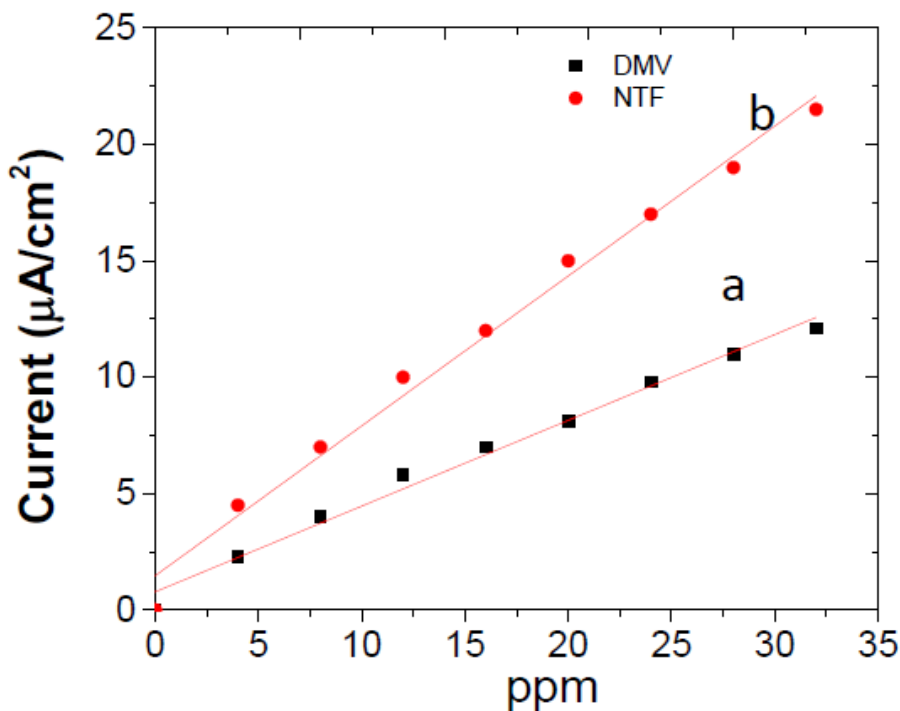


Figure 9. Calibration plot of DMV (a) and NTF (b), accumulation potential: -0.32 V; square wave frequency 60 Hz; pulse amplitude 50mV; scan rate: 20 mV s^{-1} .

The calibration curve for DMV and NTF at pH 6.0 BR buffer was measured by square wave voltammetry. The best parameters on the RGO/CS coated GCE were an accumulation time of 100 s and scan rate of 20 mV s⁻¹. SW voltammograms at different concentrations of RGO/CS/GCE were recorded using their maximum signal conditions and the curves were given in Fig. 8. The voltammetric peak current linearly increased with concentration from 0.04 to 30 µg mL⁻¹ with a slope of 0.04, 0.036 µA (r = 0.9962) and an intercept of 0.03, 0.032 µA (r= 0.9968) respectively. The calibration plots of *i*_p versus concentration lead to good linear correlation at RGO/CS/GCE (Fig. 9). The limit of detection was determined as 0.036 µg mL⁻¹ for DMV and 0.044 µg mL⁻¹ NTF on RGO/CS/GCE respectively. The relative standard deviation (RSD) of >1.8% for DMV and NTF (n=5) showed good reproducibility. The modified RGO/CS/GC electrode was used every day and stored at room temperature.

5. CONCLUSION

The described RGO/CS modified GCE was provided to be suitable for selective determination of DMV and NTF in food and environmental samples. The modified electrode was investigated by cyclic voltammetry and square wave voltammetry. It exhibits high sensitivity, less influence of matrix effect and good selectivity towards the determination of DMV and NTF. The accuracy and precision of the present method was checked by the analysis of DMV and NTF pesticide in known amount of food and environmental samples. The existing method was successfully applied for the determination of DMV and NTF in food and environmental samples. The developed modified electrode has good sensitivity, stability and dynamic linear concentration ranges with low limit of detection for the application of OPs.

References

1. X. Zhang, H.B. Wang, C.M. Yang, D. Du and Y.H. Lin, *Biosens. Bioelectron.*, 41 (2013) 669.
2. A. Sahin, K. Dooley, D.M. Cropek, A.C. West and S. Banta, *Sens. Actuators B: Chem.* 158 (2011) 353.
3. T. Liu, H.C. Su, X.G. Qu, P. Ju, L. Cui and S.Y. Ai, *Sens. Actuators B: Chem.*, 160 (2011) 1255.
4. C. Wang, Q.H. Wu, C.X. Wu and Z. Wang, *J. Sep. Sci.*, 34 (2011) 3231.
5. C. Raman Suri, R. Boro, Y. Nangia, S. Gandhi, P. Sharma, N. Wangoo, K. Rajesh and G. Shekhawat, *TrAC-Trend. Anal. Chem.*, 28 (2009) 29.
6. W. W. Ibrahim, S. M. Monjurul alam and A. B. Sulaiman, *Jurnal Teknologi*, 41(C) (2004) 1.
7. J.M. Abad, F. Pariente, L. Hernández, H.D. Abruna and E. Lorenzo, *Anal. Chem.* 70 (1998) 2848.
8. D. Du, M.H. Wang, J. Cai, Y. Tao, H.Y. Tu and A.D. Zhang, *Analyst.*, 133 (2008) 1790.
9. P. Grasso, E. Benfenati, M. Terreni, M. Pregnolato, M. Natangelo and G. Pagani, *J.Chromatogr.A*, 822 (1998) 91.
10. D. Ho Kim, G. Suk Heo and D. Woon Lee, *J.Chromatogr.A*, 824 (1998) 63.
11. O. Agrawal, J.V. Das and V.K. Gupta, *Chem. Anal.*, 43 (1998) 969.
12. F. Hernandez, R. Serrano, E. Pitarch and F. J.Lopez, *Anal.Chim.Acta*, 374 (1998) 215.
13. M. L. Cano, J. L. Vidal, F. J. E. Gonzalez, M. M. Galeza and M. C. Marquez, *Anal.Chim.Acta*, 423 (2000)127.

14. S. Hassoon and I. Schechter, *Anal. Chim. Acta*, 405 (2000) 9.
15. J. A. Perez-Serradilla, J. M. Mata-Granados and M.D.L. de Castro, *Chromatographia*, 71 (2010) 899.
16. M. K. Chai and G. H. Tan, *Food Chem.*, 117 (2009) 561.
17. T. Perez-Ruiz, C. Martinez-Lozano, V. Tomas and J. Martin, *Anal. Chim. Acta*, 540 (2005) 383.
18. C.P. Sanz, R. Halko, Z.S. Ferrera and J.J.S. Rodriguez, *Anal. Chim. Acta*, 524 (2004) 265.
19. P.R. Prasad, E.B. Naidoo and N.Y. Sreedhar, *Arabian Journal of Chemistry*, DOI: 10.1016/j.arabj.2015.02.012.
20. L.G. Rice, *J. Chromatogr.*, 317 (1984) 523.
21. M. Subbalakshamma and S.J. Reddy, *Electroanalysis*, 6 (1994) 521.
22. G. Madhavi, P.R.K. Reddy and S.J. Reddy, *Bulletin Electrochem.*, 11 (1995) 490.
23. P.T. Kissinger and W.R. Heineman, *Laboratory Techniques in Electroanalytical Chemistry*, 2nd ed., Marcel Dekker, New York (1996).
24. J. Wang, *Electroanalytical Chemistry*, 2nd ed., John Wiley and Sons, New York (2000).
25. S. Iijima, *Nature*, 354 (1991) 56.
26. M.E.G. Lyons, *Int. J. Electrochem. Sci.*, 4 (2009) 77.
27. F. Berti, L. Lozzi, I. Palchetti, S. Santucci and G. Marrazza, *Electrochim. Acta*, 54, (2009) 5035.
28. S. Park and R.S. Ruoff, *Nat. Nanotechnol.*, 4 (2009) 217.
29. S. Stankovich, D. A. Dikin, R.D. Piner, K.A. Kohlhaas, A. Kleinhammes, Y. Jia, Y. Wu, S. T. Nguyen and R. S. Ruoff, *Carbon*, 45 (2007) 1558.
30. H.C. Schniepp, J.L. Li, M.J. McAllister, H. Sai, M. Herrera-Alonso, D. H. Adamson, R.K. Prud'homme, R. Car, D. A. Saville and I. A. Aksay, *J. Phys. Chem. B*, 110 (2006) 8535.
31. H.L. Guo, X.F. Wang, Q.Y. Qian, F.B. Wang and X. H. Xia, *ACS Nano*, 3, (2009) 2653.
32. M. Zhou, Y. Wang, Y. M. Zhai, J. F. Zhai, W. Ren, F. A. Wang and S. J. Dong, *Chem. Eur. J.*, 15, (2009) 6116.
33. G. K. Ramesha and S. Sampath, *J. Phys. Chem. C*, 113 (2009) 7985.
34. J. Dong, H. Zhao, F. Qiao, P. Liu, X. Wang and S. Ai, *Anal. Methods*, 5 (2013) 2866.
35. W. Yazhen, Q. Hongxin, H. Siqian, X. Junhui, *Sensors and Actuators B Chemical*, 147 (2) (2010) 587.
36. L. Chen, Y. Tang, K. Wang, C. Liu and S. Luo, *Electrochemistry Communications*, 13 (2011) 133.
37. Q. Cheng, J. Tang, J. Ma, H. Zhang, N. Shinya and L. Qin, *Carbon*, 49 (2011) 2917.
38. M. Xu, J. Zhu, H. Su, J. Dong, S. Ai and R. Li, *J. Appl. Electrochem.*, 42 (2012) 509.
39. J. Gong, X. Miao, T. Zhou and L. Zhang, *Talanta*, 85 (2011) 1344.
40. S. Wu, X. Lan, L. Cui, L. Zhang, S. Tao, H. Wang, M. Han, Z. Liu and C. Meng, *Anal. Chim. Acta*, 699 (2011) 170.
41. J. Gong, X. Miao, H. Wan and D. Song, *Sens. Actuators B*, 162 (2012) 341.
42. Q. Zhou, L. Yang, G. Wang and Y. Yang, *Biosensors and Bioelectronics*, 49 (2013) 25.